Can the Resonance Raman Optical Activity Spectrum Display Sign Alternation?

Luciano N. Vidal,[†] Tommaso Giovannini,[‡] and Chiara Cappelli[*,‡]

Universidade Tecnológica Federal do Paraná, Rua Dep. Heitor de Alencar Furtado, 4900, 81280-340, Curitiba, Brazil, and Scuola Normale Superiore, Piazza dei Cavalieri 7, 56126 Pisa, Italy

E-mail: chiara.cappelli@sns.it

[*]To whom correspondence should be addressed

[†]Universidade Tecnológica Federal do Paraná, Rua Dep. Heitor de Alencar Furtado, 4900, 81280-340, Curitiba, Brazil

[‡]Scuola Normale Superiore, Piazza dei Cavalieri 7, 56126 Pisa, Italy

Abstract

The monosignate character of Resonance Raman Optical Activity (RROA) spectra has been often taken as granted in experimental and computational approaches, on the basis of basic theoretical approximations only considering resonance with a single electronic state of the molecule and the scattering process to be governed by the Franck-Condon mechanism. We show in this letter for the first time that, by resorting to a fully Quantum Mechanical (QM) methodology able to take into account all terms entering the general definition of RROA, and which considers excited state interference and Herzberg-Teller effects, sign alternation and at the same time intensity enhancement in RROA spectra is obtained. Such features constitute an important milestone towards the exploration of RROA of a wide range of chiral biological molecules.

Graphical TOC Entry

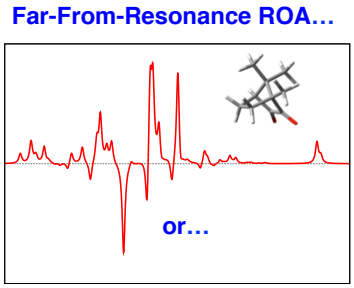

Raman optical activity (ROA),[1–4] i.e. the measure of the difference in the Raman scattering of left and right circularly polarized light, has gained increasing interest recently as valuable tools for assigning molecular absolute configurations and for obtaining information on the local environment of oscillating modes of molecular systems and especially biomolecules.[5,6] One of the recognized shortcomings of ROA is the weakness of its signal, which may prevent the experimental study of some systems or the investigation of specific spectral regions. Besides the improvement of instruments which has been reported in recent years,[7] strategies for enhancing the ROA signal have been identified, such as the creation of supramolecular structures,[8–10] interaction with metal nanoparticles,[11,12] and especially taking advantage of resonance effects.[13–18] Experiments performed in the resonance regime, *i.e.* when the frequency of the incident radiation in an ROA measurement coincides with an allowed electronic transition of the system, give rise to the so-called Resonance Raman Optical Activity (RROA),[19,20] which benefit from an increase in the ROA signal with respect to the far from resonance response. Nevertheless, the potentialities of RROA remain to date almost unexplored, and only a few measurements have been reported in the literature.[13–15] One possible cause of this situation may be due to the fact that the currently available ROA instruments[2] are designed to work in the visible region of the spectrum (532, 514 or 488 nm), where most of organic molecules do not absorb. Recently, however, a novel ROA instrument, operating in the deep-UV range of the spectrum (244 nm) has been designed,[7] and this would most probably pave the way to the extensive detection of RROA, thus enormously widening its applicability. In parallel to the lack of extensive experimental evidence of RROA, there is also a scarcity of computational approaches to calculate RROA spectra.[21,22] Because the interpretation of any ROA signal and the assignment of the spectra greatly benefit from the comparison with calculations, the lack of accurate yet generally applicable computational methodologies, has contributed to limit the investigations on this technique. A step towards this direction has been done by some of us,[23] through the definition of a novel computational methodology, accounting for Franck-Condon (FC), Herzberg-Teller (HT) and

interference effects within a formulation ensuring the independence of the calculated results among the choice of the system coordinates.

According to the theoretical fundamentals of RROA[19,23] in general there is not any simple relation between the intensities of resonance Raman (RR) and RROA spectral bands. However, in the particular case that the incident radiation is in strong resonance with a single electronic state (SES) of the molecule and the scattering process is governed by the FC mechanism, the intensities of the RROA bands are identical to the corresponding bands in the parent RR spectrum, as demonstrated by the following equation (see Section S1 given in the Supporting Information (SI) for more details):[2,19,23]

$$I_{\mathrm{RROA}}^{\mathrm{ICP}} \;=\; -\frac{1}{2} g_{rg}\; I_{\mathrm{RR}}^{\mathrm{ICP}} \tag{1}$$

where g_{rg} is the so-called *anisotropy ratio*, i.e. the ratio of electronic circular dichroism (ECD) intensity to the corresponding UV-vis absorption intensity for the transition from the ground electronic state g to the resonance state r.

Equation 1 has a relevant consequence: the RR spectrum is by definition monosignate, and within this approximation also the corresponding RROA spectrum will not display any sign alternation. This feature of the RROA has been taken as a dogma: whenever a ROA spectrum is reported to be monosignate, this is interpreted as being RROA, and most important, in case sign alternation is detected, the possible occurrence of resonance effects is not properly considered.[2,13–15,19] It is also to notice that in the early days of the development of ROA,[3] such monosignate spectra were usually rejected and interpreted as due to the polarization artifacts to which ROA was especially susceptible before the modern ROA instrument was introduced.[2]

Because it is the sign of the chiroptical response and not its absolute value, the most valuable information which can be taken from spectra in order to assign the chiral absolute configuration and study chiral molecules, the assumption of RROA being monosignate has

strongly limited its development from both the experimental and theoretical point of views. In this letter we show for the first time, by resorting to a computational modeling rooted in quantum-mechanics (QM) and going beyond the common assumptions exploited to model RROA, that the equivalence "sign alternation = far from resonance ROA" has not to be taken as granted.

There are basically two alternative mechanisms which can give rise to sign alternation in RROA: i) interference between multiple electronic excited states within the FC approximation and ii) Herzberg-Teller effects.[2,19,23] The results of these two mechanisms in the calculation of RROA spectra are illustrated in this letter.

Notice that sign alternation in RROA can also have unphysical origins due to the origin dependence of the RROA intensities when two or more non-degenerate excited states are included in the calculation of the FC RROA polarizabilities.[23] Differently from the far-from-resonance ROA, where origin dependence can be removed by using the velocity representation of the electric operators[24] or Gauge Including Atomic Orbitals,[25,26] the multi-state FC RROA spectrum evaluated through the velocity representation requires a common vertical excitation frequency to be used with the dipole and quadrupole transition moments of the different electronic states to completely cancel origin effects.[23] For this reason, all FC spectra reported in this communication were evaluated with this additional care to remove any origin dependence in the RROA cross sections. Also, sign alternation has been observed routinely in RROA spectra induced by a static magnetic field in achiral samples.[3,27,28]

As already mentioned above, sign alternation in ROA can result from the interferential features of multiple excited electronic states into the ROA tensors: in this case, no simple relation between Raman and ROA intensities can be obtained beyond the SES limit. In order to establish a relation between RROA and RR intensities, the electric dipole transition moment is assumed to be parallel to one of the coordinate axis. However, the spatial orientation of the electronic transition moments cannot be predicted from the electronic structure of the system in a simple way and there are not enough geometrical constraints to relate Raman

and ROA intensities even when only two excited states are relevant to the light scattering through the A-term FC mechanism (Equation S1 given as SI requires the FC approximation and the transition polarizability $\boldsymbol{\alpha}^{fi}$ with a single non-zero component to be valid).[2,14] For a system where the incident excitation radiation is in strong resonance with two excited states and the vibronic coupling is negligible, geometrical constraints can be used to show that there are at most five non-zero components of the transition polarizability $\boldsymbol{\alpha}^{fi}$ in general.[14] In this case, the non-zero components of the transition polarizability $\boldsymbol{\alpha}^{fi}$ are of the type: $\alpha^{fi}_{\rho\rho}$, $\alpha^{fi}_{\sigma\sigma}$ and $\alpha^{fi}_{\rho\sigma} = \alpha^{fi}_{\sigma\rho}$, with $\rho \neq \sigma$ and ρ,σ being one of the Cartesian directions. Therefore, the corresponding RR and RROA intensities are not simply related and the sign of each RROA band will depend not only on the spatial orientation of the transition moments but also on the magnitude of each non-zero component of the ROA tensors. Because these magnitudes are peculiar to each vibrational transition, sign alternation can occur in this type of RROA scattering.

The occurrence of sign alternation when the incident radiation is simultaneously in resonance with two excited states is illustrated on the left panel of Figure 1, which shows the RROA spectrum of (1R)-camphorquinone in cyclohexane solution. The corresponding RR and Circular Intensity Difference (CID)[2,3] spectra are given in Figure S1 in the SI. This spectrum was obtained by using the B3LYP exchange-correlation functional[29] and the polarized double-ζ SNSD basis set,[30,31] while solvent effects are described with the Polarizable Continuum Model (PCM).[32] All the calculations reported in this letter were performed by using a locally modified version of the Gaussian package.[33] The RR and RROA polarizabilities were evaluated for the S_5 and S_6 singlet excited states (λ_{S5}=214 nm, λ_{S6}=211 nm), see also Table S1 in the SI) using the velocity representation of the electric dipole and traceless quadrupole, at the excitation wavelength $\lambda_0 = 217$ nm and with the dumping factor $\Gamma = 350$ cm^{-1} for both excited states. The vertical excitation energies, oscillator and rotational strengths of the S_5 and S_6 states are reported in Table S1 of the SI. Excited state Potential Energy Surfaces (PES) were represented by the Vertical Gradient (VG) model.[34,35] According to

reference 2, the strong resonance limit in RR and RROA occurs when the frequency of the incident photon closely matches the frequency of a particular electronic/vibronic transition, such that $\omega_{rg} + \omega_{ni} - \omega_0 \approx 0$, in Equations (S3) and (S4). Within the VG model, the energy of the 0–0 vibronic transition is simply the difference between the ground and excited state electronic energies taken from the respective minima of each PES (such energy corresponds to $\hbar\omega_{rg}$). For instance, if $\omega_0 - \omega_{rg}$ is equal to the frequency of one normal vibration in the ground electronic state, there will be a perfect cancelation of the corresponding $\omega_{rg} + \omega_{ni} - \omega_0$ term where the intermediate vibrational state differs only by plus one unit in the quantum number of that particular normal mode with respect to the initial vibrational state, *i.e.* $\boldsymbol{n^r} - \boldsymbol{i^g} = (0, \cdots, 0, 1, 0, \cdots, 0)$, with $\boldsymbol{n^r}$ and $\boldsymbol{i^g}$ being vectors defining the initial and intermediate vibrational states. All spectra reported in this work were convoluted with Lorentzian functions having a full width at half maximum of 10 cm^{-1} and the absolute RROA intensities are given in terms of differential cross sections for the unpolarized backscattering Scattered Circular Polarization (SCP) ROA which also obeys Equation S1 in SI at the SES limit. From Figure 1 it is evident that sign alternation is possible. Also, the strongest RROA bands of (1R)-camphorquinone have a negative sign.

Sign alternation is also expected in case RROA polarizabilities are evaluated with three or more A-terms (FC level).[2] This mechanism is illustrated by the right panel of Figure 1, which reports RROA spectra of (S)-nicotine in aqueous solution calculated by considering states S_1, S_2 and S_3 (for conformer A: λ_{S1}=240 nm, λ_{S2}=231 nm, λ_{S3}=228 nm, for conformer B: λ_{S1}=242 nm, λ_{S2}=229 nm, λ_{S3}=228 nm, see also Table S2 in SI) and excitation wavelengths of λ_0 = 238 nm and λ_0 = 250 nm. The corresponding RR and CID spectra are show by Figure S4 in the SI. By following previous studies on this molecule performed by some of us,[36,37]the CAM-B3LYP/aug-cc-pVDZ level of theory was exploited. Solvent effects (aqueous solution) were described by means of the PCM. At 298.15 K, (S)-nicotine exists in two stable conformers (see Figure S3 in the SI) with the thermal population of conformer A being equal to 55.3%.[36] The vertical excitation wavelengths for the first three singlet excited states of

conformers A and B lie in the range of $242-228$ nm and the rotatory strength is negative for S_1 and positive for S_2 and S_3 for both A and B conformers (Table S2 in SI).[36] Interestingly, for the excitation wavelength lying within the absorption bands ($\lambda_0 = 238$ nm) there is no sign alternation in the RROA spectrum. Nevertheless, when the excitation wavelength is in the pre-resonance regime ($\lambda_0 = 250$ nm) strong sign alternation is observed (the corresponding RR and CID spectra are show by Figure S5 in the SI). Therefore, absence of sign alternation in RROA does not necessarily implies a single excited state scattering, as it is always the case within the SES limit.

For those systems where only a single excited state is in strong resonance with the excitation radiation it is still possible to observe sign alternation in RROA due to the Herzberg-Teller (HT) vibronic coupling mechanism.[2,23,38,39] The FC approximation is expected to work well for RR if the electronic transition is strongly allowed at the excitation frequency λ_0 or close enough to that wavelength.[34,40] On the other hand, since RROA intensities depend on the magnitude of the the transition tensors $\boldsymbol{G}^{fi}$ and $\boldsymbol{\mathcal{G}}^{fi}$,[23] even if at the simplest level of theory, i.e. SES, if the electric and magnetic transition moments are individually large, they may be oriented in such a way that the rotational strength is small, so that small resonance enhancement for the RROA intensities will occur. Under such circumstances, where the A-term tensors of RROA are not large, the contribution of other excited states to the RROA scattering through the HT intensity-borrowing mechanism can introduce non-negligible corrections to the RROA tensors.[23] The simplest theory that allows for the inclusion of HT effects is the so called Two Excited States B-term model (TES-B) where two excited states, with at least one of them being in resonance with the excitation radiation, interact with each other through the vibronic coupling between them.[2] Since the TES-B model involves an additional excited state with respect to the SES limit, there are not enough geometrical constraints to fulfill the requirements of $\boldsymbol{\alpha}^{fi}$ having all but one non-zero component necessary for the validity of Equation S1 in SI. At the HT level, the dependence of the electric dipole transition moment on the nuclear coordinates is usually expressed in terms

of the linear term in the Taylor expansion of this property with respect to the normal coordinates.[34,40] From that expansion, by using perturbation theory, it is possible to show that *all* the excited states (not only two) make a contribution to the geometrical derivatives of the transition moment.[35] Supposing that the scattering system is oriented so to have its electric dipole transition moment at the ground state equilibrium geometry parallel to the z-axis, the molecular vibrations can introduce contributions to that property in other than its z-component, due to the non-totally symmetric normal modes, in those molecules with some point group symmetry, or from all normal modes if the chiral molecule belongs to the C_1 group. The relevance of the HT coupling to the transition moment itself will depend on the magnitude of its first derivative with respect to each normal mode, according to the following expansion:[35]

$$\mu_\rho^{gr} = \delta_{\rho z}\mu_{\rho,0}^{gr} + \sum_k \mu_{\rho,k}^{gr} Q_k^g + \text{high order terms} \tag{2}$$

where μ_ρ^{gr} is the ρ-component of the electric dipole transition moment between states g and r at arbitrary geometries. $\mu_{\rho,0}^{gr}$ is the same quantity at the equilibrium geometry (where only its z-component is non-zero), $\delta_{\rho z}$ is 1 for $\rho = z$ and 0 otherwise, $\mu_{\rho,k}^{gr}$ is the first derivative of μ_ρ^{gr} with respect to the ground state normal coordinate Q_k^g. Nonetheless, the importance of the HT mechanism for each RROA transition will depend, in addition to the value of the above derivatives, also on the value of the HT integrals for that particular vibrational transition. According to equation 2, any of the nine components of $\boldsymbol{\alpha}^{fi}$ can be different from zero. Furthermore, the resulting RR and RROA polarizabilities are not symmetric anymore, due to the form of the HT integrals. Therefore, the four anti-symmetric anisotropic rotational invariants of RROA can now contribute to the RROA intensities, as well as the RR intensities will receive a contribution from the anti-symmetric anisotropic invariant of $\boldsymbol{\alpha}^{fi}$. From the above considerations we see that at the HT level one returns to the most general theory of ROA scattering, where sign alternation is always possible and therefore one should not

expect a mono-signate RROA spectrum to be a rule at this level of theory.

To illustrate this, following a similar computational protocol as in the FC RROA calculations, the HT RROA spectrum of (1R)-camphorquinone in cyclohexane was computed for state S_1 (λ_{S1}=499 nm, see also Table S1 in SI) using the Adiabatic Hessian (AH) PES model[34,35] and an excitation wavelength $\lambda_0 = 545$ nm corresponding to the 0–0 vibronic energy. The HT RROA spectrum is shown on the left panel of Figure 2 together with the FC spectrum. In this molecule, the S_2 state is predicted to be far apart from S_1, lying in the UV region (295 nm for the vertical excitation, see table S1 in SI). The rotatory strength for state S_1 is -1.4×10^{-40} erg.esu.cm.Gauss^{-1} and thus, the FC RROA presents only positive peaks, as expected. On the other hand, when the vibronic coupling is taken into account, there is a significant increase in the intensity of several bands and, in addition, there are many peaks with negative sign. Furthermore, on the right panel of Figure 2 the HT-RROA spectrum of (1R)-camphorquinone is compared with the far-from-resonance ROA spectrum obtained with $\lambda_0 = 1064$ nm. Clearly, one cannot distinguish which one is the resonance spectrum based on the single-sign criteria but, as usual, there is the characteristic resonance enhancement of some bands and the RROA intensities are about two orders of magnitude stronger at $\lambda_0 = 545$ nm, though part of this increasing is due to the fourth power dependency in the cross sections. Notice that, at the HT level, a single excited state RROA scattering suffers from origin dependence and special care must be taken to evaluate the corresponding RROA intensities. In order to completely remove origin effects from the RROA spectrum the rotational invariants of the quadrupole tensors were calculated with the modifications suggested in a previous study of some of us.[23] The corresponding calculated RR and Circular Intensity Difference (CID)[2,3] spectra for the S_1 state of (1R)-camphorquinone excited at $\lambda_0 = 545$ nm are given in Figure S2 in the SI. The simple relation between RROA and RR intensities described by Equation 1 is explicitly evidenced by the blue line in the CID spectrum.

In conclusion, we have shown in this letter for the first time that, by resorting to a fully QM

methodology able to take into account all terms entering the general definition of RROA, and which considers excited state interference and HT effects, sign alternation and at the same time intensity enhancement in RROA spectra is obtained. Our findings, in combination with a recent breakthrough in ROA instrumentation,[7] allowing measurement in the deep UV range not plagued by interfering residual fluorescence, will boost the interest in RROA, and constitute an important milestone in the exploration of resonance ROA scattering phenomena of a wide range of interesting biological molecules.

Acknowledgements

CC acknowledge support from the Italian MIUR (PRIN 2012 NB3KLK002) and COST CMST-Action CM1405 MOLecules In Motion (MOLIM). The HPC computational facilities available at the SMART@SNS Lab are also acknowledged.
LNV thanks to Conselho Nacional de Desenvolvimento Científico e Tecnológico - Brasil for the financial support (Grant No. 231199/2013-9).

Supporting Information Available

Theory of Single-Excited State-Franck-Condon (SES-FC) RROA. Definition of RROA transition polarizabilities at the Franck-Condon and Herzberg-Teller levels. Description of the computational procedure exploited to the reported results. Tables of vertical excitation energies, oscillator and rotatory strengths for (1R)-camphorquinone and (S)-Nicotine. Structure of the two most representative conformers of (S)-nicotine. Resonance Raman and Circular Intensity Difference (CID) spectra of (R)-Camphorquinone and (S)-Nicotine for selected incident frequencies.

References

(1) Barron, L. D.; Bogaard, M. P.; Buckingham, A. D. Raman Scattering of Circularly Polarized Light by Optically Active Molecules. *J. Am. Chem. Soc.* **1973**, *95*, 603–605.

(2) Nafie, L. A. *Vibrational Optical Activity*; John Wiley & Sons: Chichester, 2011.

(3) Barron, L. *Molecular Light Scattering and Optical Activity*, 2nd ed.; Cambridge University Press: New York, 2004.

(4) Barron, L. D.; Buckingham, D. A. Vibrational Optical Activity. *Chem. Phys. Lett.* **2010**, *492*, 199–213.

(5) Barron, L. D.; Hecht, L.; Blanch, E. W.; Bell, A. F. Solution Structure and Dynamics of Biomolecules from Raman Optical Activity. *Prog. Biophys. Molecular Biol.* **2000**, *73*, 1 – 49.

(6) Blanch, E. W.; McColl, I. H.; Hecht, L.; Nielsen, K.; Barron, L. D. Structural Characterization of Proteins and Viruses Using Raman Optical Activity *Vibr. Spectrosc.* **2004**, *35*, 87 – 92.

(7) Kapitán, J.; Barron, L. D.; Hecht, L. A Novel Raman Optical Activity Instrument Operating in the Deep Ultraviolet Spectral Region. *J. Raman Spectrosc.* **2015**, *46*, 392–399.

(8) Merten, C.; Barron, L. D.; Hecht, L.; Johannessen, C. Determination of the Helical Screw Sense and Side-Group Chirality of a Synthetic Chiral Polymer from Raman Optical Activity. *Angew. Chem. Int. Ed.* **2011**, *50*, 9973–9976.

(9) Kurouski, D.; Handen, J. D.; Dukor, R. K.; Nafie, L. A.; Lednev, I. K. Supramolecular Chirality in Peptide Microcrystals. *Chem. Commun.* **2015**, *51*, 89–92.

(10) Kurouski, D.; Lombardi, R. A.; Dukor, R. K.; Lednev, I. K.; Nafie, L. A. Direct Observation and pH Control of Reversed Supramolecular Chirality in Insulin Fibrils by Vibrational Circular Dichroism. *Chem. Commun.* **2010**, *46*, 7154–7156.

(11) Abdali, S.; Blanch, E. W. Surface Enhanced Raman Optical Activity (SEROA). *Chem. Soc. Rev.* **2008**, *37*, 980–992.

(12) Pour, S. O.; Rocks, L.; Faulds, K.; Graham, D.; Parchansky, V.; Bour, P.; Blanch, E. W. Through-space Transfer of Chiral Information Mediated by a Plasmonic Nanomaterial. *Nature Chemistry* **2015**, *7*, 591–596.

(13) Vargek, M.; Freedman, T. B.; Lee, E.; Nafie, L. A. Experimental Observation of Resonance Raman Optical Activity. *Chem. Phys. Lett.* **1998**, *287*, 359–364.

(14) Merten, C.; Li, H.; Lu, X.; Hartwig, A.; Nafie, L. A. Observation of Resonance Electronic and Non-resonance-enhanced Vibrational Natural Raman Optical Activity. *J. Raman Spectrosc.* **2010**, *41*, 1563–1565.

(15) Merten, C.; Li, H.; Nafie, L. A. Simultaneous Resonance Raman Optical Activity Involving Two Electronic States. *J. Phys. Chem. A* **2012**, *116*, 7329–7336.

(16) Yamamoto, S.; Bouř, P. Detection of Molecular Chirality by Induced Resonance Raman Optical Activity in Europium Complexes. *Angew. Chem. Int. Ed.* **2012**, *51*, 11058–11061.

(17) Yamamoto, S.; Bouř, P. Transition Polarizability Model of Induced Resonance Raman Optical Activity. *J. Comput. Chem.* **2013**, *34*, 2152–2158.

(18) Magg, M.; Kadria-Vili, Y.; Oulevey, P.; Weisman, R. B.; Bürgi, T. Resonance Raman Optical Activity Spectra of Single-Walled Carbon Nanotube Enantiomers. *J. Phys. Chem. Lett.* **2016**, *7*, 221–225.

(19) Nafie, L. A. Theory of Resonance Raman Optical Activity: the Single Electronic State Limit. *Chem. Phys.* **1996**, *205*, 309–322.

(20) Nafie, L. A. Theory of Raman Scattering and Raman Optical Activity: Near Resonance Theory and Levels of Approximation. *Theor. Chem. Acc.* **2008**, *119*, 39–55.

(21) Jensen, L.; Autschbach, J.; Krykunov, M.; Schatz, G. C. Resonance Vibrational Raman Optical Activity: A Time-dependent Density Functional Theory Approach. *J. Chem. Phys.* **2007**, *127*, 134101.

(22) Luber, S.; Neugebauer, J.; Reiher, M. Enhancement and De-enhancement Effects in Vibrational Resonance Raman Optical Activity. *J. Chem. Phys.* **2010**, *132*, 044113.

(23) Vidal, L. N.; Egidi, F.; Barone, V.; Cappelli, C. Origin Invariance in Vibrational Resonance Raman Optical Activity. *J. Chem. Phys.* **2015**, *142*, 174101.

(24) Luber, S.; Reiher, M. Raman Optical Activity Spectra of Chiral Transition Metal Complexes. *Chem. Phys.* **2008**, *346*, 212–223.

(25) Helgaker, T.; Ruud, K.; Bak, K. L.; Jørgensen, P.; Olsen, J. Vibrational Raman Optical Activity Calculations Using London Atomic Orbitals. *Faraday Disc.* **1994**, *99*, 165–180.

(26) Ruud, K.; Helgaker, T.; Bour, P. Gauge-origin Independent Density-functional Theory Calculations of Vibrational Raman Optical Activity. *J. Phys. Chem. A* **2002**, *106*, 7448–7455.

(27) Barron, L.; Meehan, C.; Vrbancich, J. Magnetic Resonance-Raman Optical Activity of Ferrocytochrome C Theory and Experiment. *J. Raman Spectrosc.* **1982**, *12*, 251–261.

(28) Barron, L.; Vrbancich, J. Magnetic Raman Optical Activity. *Adv. Infrared Raman Spectrosc.* **1985**, *12*, 215–272.

(29) Becke, A. D. Density-functional Thermochemistry. III. The Role of Exact Exchange. . *Chem. Phys.* **1993**, *98*, 5648–5652.

(30) Barone, V.; Biczysko, M.; Bloino, J. Fully Anharmonic IR and Raman Spectra of Medium-size Molecular Systems: Accuracy and Interpretation. *Phys. Chem. Chem. Phys.* **2014**, *16*, 1759–1787.

(31) Double and Triple-zeta basis sets of SNS and N07 Families, are available for download. Visit http://dreamsnet.sns.it/downloads (accessed August 25, 2016).

(32) Tomasi, J.; Mennucci, B.; Cammi, R. Quantum Mechanical Continuum Solvation Models. *Chem. Rev.* **2005**, *105*, 2999–3094.

(33) Frisch, M. J.; Trucks, G. W.; Schlegel, H. B.; Scuseria, G. E.; Robb, M. A.; Cheeseman, J. R.; Scalmani, G.; Barone, V.; Mennucci, B.; Petersson, G. A.; Nakatsuji, H.; Caricato, M.; Li, X.; Hratchian, H. P.; Izmaylov, A. F.; Bloino, J.; Janesko, B. G.; Lipparini, F.; Zheng, G.; Sonnenberg, J. L.; Liang, W.; Hada, M.; Ehara, M.; Toyota, K.; Fukuda, R.; Hasegawa, J.; Ishida, M.; Nakajima, T.; Honda, Y.; Kitao, O.; Nakai, H.; Vreven, T.; Montgomery, J. A.; Jr.,; Peralta, J. E.; Ogliaro, F.; Bearpark, M.; Heyd, J. J.; Brothers, E.; Kudin, K. N.; Staroverov, V. N.; Keith, T.; Kobayashi, R.; Normand, J.; Raghavachari, K.; Rendell, A.; Burant, J. C.; Iyengar, S. S.; Tomasi, J.; Cossi, M.; Rega, N.; Millam, J. M.; Klene, M.; Knox, J. E.; Cross, J. B.; Bakken, V.; Adamo, C.; Jaramillo, J.; Gomperts, R.; Stratmann, R. E.; Yazyev, O.; Austin, A. J.; Cammi, R.; Pomelli, C.; Ochterski, J. W.; Martin, R. L.; Morokuma, K.; Zakrzewski, V. G.; Voth, G. A.; Salvador, P.; Dannenberg, J. J.; Dapprich, S.; Parandekar, P. V.; Mayhall, N. J.; Daniels, A. D.; Farkas, O.; Foresman, J. B.; Ortiz, J. V.; Cioslowski, J.; Fox, D. J. Gaussian Development Version, Revision H.37+. Gaussian, Inc., Wallingford CT, 2010.

(34) Egidi, F.; Bloino, J.; Cappelli, C.; Barone, V. A Robust and Effective Time-independent Route to the Calculation of Resonance Raman Spectra of Large Molecules in Condensed Phases with the Inclusion of Duschinsky, Herzberg-Teller, Anharmonic, and Environmental Effects. *J. Chem. Theory Comput.* **2014**, *10*, 346–363.

(35) Barone, V., Ed. *Computational Strategies for Spectroscopy*; John Wiley & Sons: New Jersey, 2012.

(36) Egidi, F.; Russo, R.; Carnimeo, I.; D'Urso, A.; Mancini, G.; Cappelli, C. The Electronic Circular Dichroism of Nicotine in Aqueous Solution: A Test Case for Continuum and Mixed Explicit-Continuum Solvation Approaches. *J. Phys. Chem. A* **2015**, *119*, 5396–5404.

(37) Egidi, F.; Segado, M.; Koch, H.; Cappelli, C.; Barone, V. A Benchmark Study of Electronic Excitation Energies, Transition Moments, and Excited-state Energy Gradients on the Nicotine Molecule. *J. Chem. Phys.* **2014**, *141*, 224114.

(38) Herzberg, G.; Teller, E. Schwingungsstruktur der Elektronenübergänge bei mehratomigen Molekülen. *Z. Phys. Chem. B* **1933**, *21*, 410.

(39) Long, D. A. *The Raman Effect: A Unified Treatment of the Theory of Raman Scattering by Molecules*; John Wiley & Sons Ltd : New York, 2002.

(40) Santoro, F.; Cappelli, C.; Barone, V. Effective Time-Independent Calculations of Vibrational Resonance Raman Spectra of Isolated and Solvated Molecules Including Duschinsky and Herzberg-Teller Effects. *J. Chem. Theory Comput.* **2011**, *7*, 1824–1839.

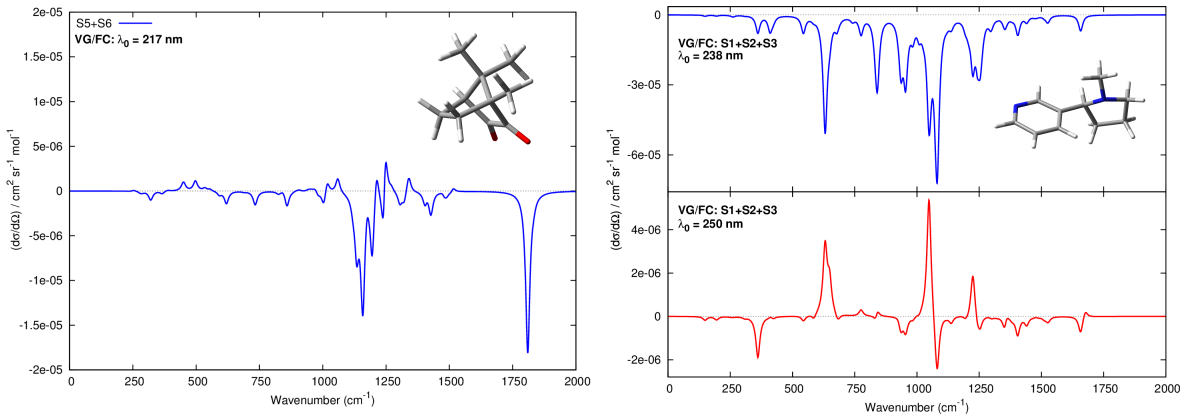

(a) **(b)**

Figure 1: VG/FC RROA spectra of **(a)** (1R)-camphorquinone in cyclohexane and **(b)** (S)-nicotine in water. The excitation wavelength λ_0 and excited states used to compute the RROA polarizabilities are shown above.

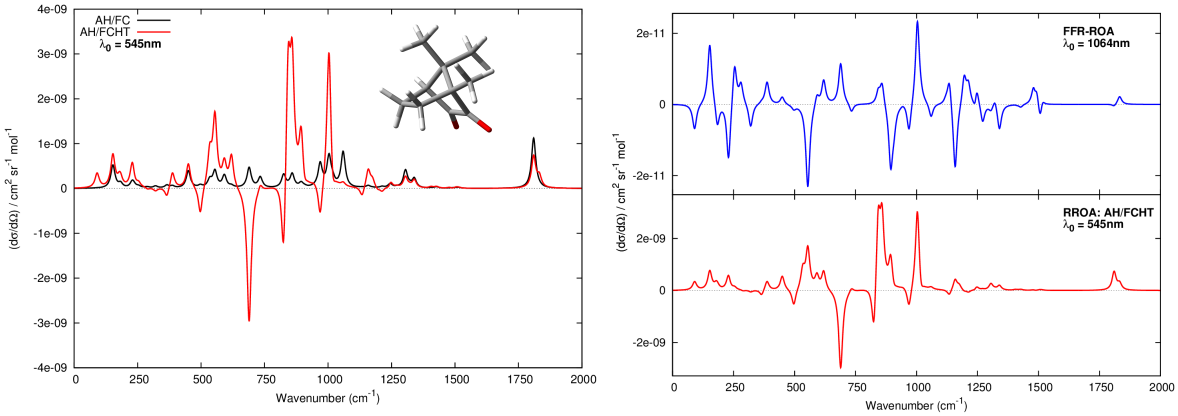

(a) **(b)**

Figure 2: AH/FC and AH/FCHT RROA spectra for the S_1 state of (1R)-camphorquinone in cyclohexane **(a)**, its far-from-resonance ROA spectrum in the same solvent **(top of b)** and its AH/FCHT RROA spectrum for state S_1 **(bottom of b)**.